Specific glucoside transporters influence septal structure and function in the filamentous, heterocyst-forming cyanobacterium Anabaena sp. strain PCC 7120.

Nieves-Morión, M; Lechno-Yossef, S; López-Igual, R; Frías, JE; Mariscal, V; Nürnberg, DJ; Mullineaux, CW; Wolk, CP; Flores, E

Specific glucoside transporters influence septal structure and function in the filamentous, heterocyst-forming cyanobacterium *Anabaena* sp. strain PCC 7120

Mercedes Nieves-Morión[1], Sigal Lechno-Yossef[2], Rocío López-Igual[1*], José E. Frías[1], Vicente Mariscal[1], Dennis J. Nürnberg[3], Conrad W. Mullineaux[4], C. Peter Wolk[2], and Enrique Flores[1#]

[1]Instituto de Bioquímica Vegetal y Fotosíntesis, CSIC and Universidad de Sevilla, Américo Vespucio 49, E-41092 Seville, Spain; [2]MSU-DOE Plant Research Laboratory, Michigan State University, East Lansing, Michigan 48824, USA; [3]Department of Life Sciences, Imperial College London, London SW7 2AZ, United Kingdom; [4]School of Biological and Chemical Sciences, Queen Mary University of London, Mile End Road, London E1 4NS, United Kingdom.

Running head: Glucoside transporters in *Anabaena*

#Address correspondence to Enrique Flores, eflores@ibvf.csic.es.

*Present address: Institut Pasteur, Unité Plasticité du Génome Bactérien, Département Génomes et Génétique, CNRS, Unité Mixte de Recherche 3525, F-75015 Paris, France

Key words: Cyanobacteria; Glucoside transport; Heterocyst; Intercellular diffusion; Membrane transporters.

ABSTRACT

When deprived of combined nitrogen, some filamentous cyanobacteria contain two cell types: vegetative cells that fix CO_2 through oxygenic photosynthesis and heterocysts that are specialized in N_2 fixation. In the diazotrophic filament, the vegetative cells provide the heterocysts with reduced carbon (mainly in the form of sucrose) and heterocysts provide the vegetative cells with combined nitrogen. Septal junctions traverse peptidoglycan through structures known as nanopores, and appear to mediate intercellular molecular transfer that can be traced with fluorescent markers, including the sucrose analog esculin (a coumarin glucoside) that is incorporated into the cells. Uptake of esculin by the model heterocyst-forming cyanobacterium *Anabaena* sp. strain PCC 7120 was inhibited by the α-glucosides sucrose and maltose. Analysis of *Anabaena* mutants identified components of three glucoside transporters that move esculin into the cells: GlsC (Alr4781) and GlsP (All0261) are, respectively, an ATP-binding subunit and a permease subunit of two different ABC transporters, and HepP (All1711) is a major facilitator superfamily (MFS) protein that was shown previously to be involved in formation of the heterocyst envelope. Transfer of fluorescent markers (especially calcein) between vegetative cells of *Anabaena* was impaired by mutation of glucoside transporter genes. GlsP and HepP interact in bacterial two-hybrid assays with the septal junction-related protein SepJ, and GlsC was found to be necessary for formation of a normal number of septal peptidoglycan nanopores and for normal subcellular localization of SepJ. Therefore, beyond their possible role in nutrient uptake in *Anabaena*, glucoside transporters influence the structure and function of septal junctions.

Journal of Bacteriology JB Journal of Bacteriology

IMPORTANCE

Heterocyst-forming cyanobacteria have the ability to perform oxygenic photosynthesis and to assimilate atmospheric CO_2 and N_2. These organisms grow as filaments that fix these gases specifically in vegetative cells and heterocysts, respectively. For the filaments to grow, these types of cells exchange nutrients including sucrose, which serves as a source of reducing power and of carbon skeletons for the heterocysts. Movement of sucrose between cells in the filament takes place through septal junctions and has been traced with a fluorescent sucrose analog, esculin, that can be taken up by the cells. We here identified α-glucoside transporters of *Anabaena* that mediate uptake of esculin and, notably, influence septal structure and the function of septal junctions.

INTRODUCTION

Filamentous cyanobacteria of the orders Nostocales and Stigonematales fix atmospheric nitrogen in specialized cells called heterocysts (1). Heterocysts are formed from vegetative cells when the filaments of those cyanobacteria lack a source of combined nitrogen (2). The heterocysts provide the vegetative cells with fixed nitrogen, and the vegetative cells, which fix carbon dioxide through oxygenic photosynthesis, provide the heterocysts with reduced carbon (3). Substances exchanged between the two cell types include regulators such as PatS- and HetN-derived peptides and nutrients including amino acids and sugars (4). In the model heterocyst-forming cyanobacterium *Anabaena* sp. strain PCC 7120 (hereafter *Anabaena*) grown in the absence of combined nitrogen, heterocysts constitute about 10% of the cells and are distributed with a semi-regular pattern along the filament (2). This implies that one heterocyst feeds more than one vegetative cell with fixed nitrogen. Two routes have been considered for intercellular molecular transfer, the continuous periplasm of the filament (5, 6) and cell-cell joining structures (7), now termed septal junctions (8-10). The latter would represent a kind of symplasmic route (11) implying intercellular transfer between vegetative cells as well as between heterocysts and vegetative cells.

Proteins SepJ, FraC and FraD that are located at the cell poles in the intercellular septa of the filaments of *Anabaena* are integral membrane proteins (12, 13). SepJ and FraD have predicted extra-membrane domains that appear to reside in the periplasm (10, 14-16). Intercellular molecular exchange in the cyanobacterial filament can be traced with fluorescent markers including calcein, 5-carboxyfluorescein (5-CF) and esculin, and transfer has been found to be impaired in inactivated mutants of *sepJ*, *fraC* and *fraD* (7, 14, 17, 18). Additionally, perforations (termed nanopores) that have been observed in septal peptidoglycan disks from heterocyst-forming cyanobacteria (19) are present at decreased numbers in those mutants (18). Structures observed by electron tomography of *Anabaena* that have been termed “channels” (20) likely correspond to the nanopores. SepJ, FraC and FraD appear to contribute to the formation of cell-cell joining structures (septal junctions) that traverse the septal peptidoglycan through the nanopores. Differential impairment in the transfer of calcein and 5-CF in the

sepJ and *fraC-fraD* mutants has suggested that two types of septal junction complexes exist, one related to SepJ and another related to FraCD (14).

Sucrose appears to be a quantitatively important metabolite transferred from vegetative cells to heterocysts (21-25). Intercellular transfer of sucrose has been probed in *Anabaena* using esculin (6,7-dihydroxycoumarin β-D-glucoside), a fluorescent analog of this sugar (18). Esculin is taken up into the cells by a mechanism that can be inhibited by the presence of sucrose. Once inside the cells, esculin can be transferred cell-to-cell in the filament by diffusion through the septal junctions (18, 26). Thus, septal junctions are functionally analogous to the gap junctions of metazoans (18, 26).

In this work, we addressed the transporters that are involved in esculin uptake in *Anabaena* and their role, if any, in intercellular molecular transfer. The genome of *Anabaena* contains several open reading frames predicted to encode components of sugar transporters (27). We have identified three genes that are involved in uptake of esculin, two that encode components of two different ABC uptake transporters and one that encodes a Major Facilitator Superfamily (MFS) transporter. We also found that the three identified glucoside transporters influence intercellular molecular exchange in *Anabaena*. One of the ABC transporter components, an ATP-binding subunit, is needed for the correct subcellular localization of SepJ, and the two other transporters appear to affect SepJ function.

MATERIALS AND METHODS

Strains and growth conditions. *Anabaena* sp. strain PCC 7120 and derivative strains (described in Table S1) were grown in BG11 medium modified to contain ferric citrate instead of ferric ammonium citrate (28) or $BG11_0$ medium (BG11 further modified by omission of $NaNO_3$) at 30ºC in the light (ca. 25-30 µmol photons m^{-2} s^{-1}), in shaken (100 r.p.m.) liquid cultures. For tests on solid medium, media BG11 or $BG11_0$ were solidified with 1% (w/v) Difco Bacto agar. For isolation of the *glsC* (*alr4781*), *glsP* (*all0261*) and *glsC glsP* mutants, *Anabaena* was grown, with shaking, in flask cultures of AA/8 liquid medium with nitrate (29), or in medium AA with nitrate solidified with 1.2% (w/v) purified (Difco) Bacto

agar (29) at 30°C and illuminated as above. When appropriate, antibiotics were added to the cyanobacterial cultures at the following concentrations: in liquid cultures—streptomycin sulfate (Sm), 2-5 μg ml^{-1}; spectinomycin dihydrochloride pentahydrate (Sp), 2-5 μg ml^{-1}; erythromycin (Em), 5 μg ml^{-1}; and neomycin sulfate (Nm), 5-25 μg ml^{-1}; and in solid media—Sm, 5-10 μg ml^{-1}; Sp, 5-10 μg ml^{-1}; Em, 5-10 μg ml^{-1}; and Nm, 30-40 μg ml^{-1}. Chlorophyll *a* (Chl) content of cultures was determined by the method of Mackinney (30).

Escherichia coli strains were grown in LB medium, supplemented when appropriate with antibiotics at standard concentrations (31). *E. coli* strains DH5α or DH5αMCR were used for plasmid constructions. *E. coli* strains DH5α or ED8654 bearing a conjugative plasmid, and strains HB101 or DH5αMCR bearing a methylase-encoding helper plasmid and the cargo plasmid, were used for conjugation with *Anabaena*, unless stated otherwise (32).

Construction of *Anabaena* mutant strains. The *alr4781* (*glsC*) mutant, DR3912a, was generated by a di-parental mating between *Anabaena* and DH5αMCR carrying pRL443, pRL3857a and pRL3912a (plasmids described in Table S1). The single recombinant was selected on Em, tested for sucrose sensitivity, and then went through a sucrose selection cycle, as described by Cai and Wolk (33), for selection of the double recombinant (Fig. S1). Similarly, a double recombinant deletion mutant of *all0261* (*glsP*), DR3915 (Fig. S1), was generated by mating between *Anabaena* and DH5αMCR carrying pRL443, pRL3857a and pRL3915. Because DR3912a and DR3915 carry the same antibiotic resistance marker (Sm^R Sp^R), a new plasmid, pRL3985a, was constructed for creation of the *glsC glsP* double mutant (Fig. S1). In this case, pRL3985a was introduced into DR3912a by conjugation, and the mutant was selected as described above.

For complementation of the *glsC* mutant (DR3912a), a fragment containing ORF *alr4781* and 202 bp of upstream and 49 bp of downstream DNA was amplified using *Anabaena* DNA as template and primers alr4781-3 and alr4781-4 (oligodeoxynucleotide primers are described in Table S1). The PCR product was cloned into vector pSpark I producing pCSMN21. This construct was verified by sequencing and transferred as a BamHI fragment to pRL25C (34) digested with the same enzyme producing

130 pCSMN22. This plasmid was transferred to DR3912a by conjugation. Clones resistant to Sm, Sp and Nm
131 were isolated and their genetic structure was verified by PCR with primers alr4781-3 and alr4781-4 (Fig.
132 S2). This strain was named CSMN11. For complementation of the *glsP* mutant (DR3915), a fragment
133 containing ORF *all0261* and 103 bp of upstream and 40 bp of downstream DNA was amplified using
134 *Anabaena* DNA as template and primers all0261-3 and all0261-4. The PCR product was cloned into
135 pSpark I producing pCSMN19, which was confirmed by sequencing and transferred as a BamHI fragment
136 to pRL25C digested with BamHI producing pCSMN20. This plasmid was transferred to DR3915 by
137 conjugation. Clones resistant to Sm, Sp and Nm were insolated and their genetic structure was verified by
138 PCR with primers all0261-3 and all0261-4 (Fig. S2). This strain was named CSMN12.

139 For inactivation of *alr3705*, an internal fragment of 560 bp was amplified by PCR using
140 *Anabaena* DNA as template and primers alr3705-1 (bearing a BamHI site in its 5' end) and alr3705-2.
141 The amplified fragment was cloned into pMBL-T (http://www.molbiolab.es/uploads/phpgSgmue.pdf;
142 Dominion MBL, Spain) and transferred as a BamHI-ended fragment (the second BamHI site is from the
143 vector multiple cloning site) to BamHI-digested pCSV3 (35) producing pCSRL49. This plasmid was
144 transformed into *E. coli* HB101 (pRL623) and transferred to *Anabaena* and to *hepP* (*all1711*) mutant
145 strain FQ163 (36) by conjugation with selection for Sm^R Sp^R (because FQ163 is itself Nm^R Sm^R
146 $bleomycin^R$, in this case effective selection is only for Sp^R). Clones that had incorporated pCSRL49 by
147 single recombination were selected for further study and named strain CSRL15 (wild-type background)
148 and CSMN3 (*hepP* background) (Fig. S3).

149 To prepare an *Anabaena* strain producing a fusion of the GFP to GlsC, a 950-bp DNA fragment
150 from the 3' region of *glsC* (*alr4781*) was amplified using *Anabaena* DNA as template and primers
151 alr4781-5 and alr4781-6. The 950-bp PCR product was cloned into pSpark I producing pCSMN23. This
152 construct was validated by sequencing and transferred to SacI-XhoI-digested pRL277 (37) as a SacI-NheI
153 fragment together with NheI-SalI-digested *gfp-mut2* (38), producing pCSMN24, in which the *gfp-mut2*
154 gene is fused to *glsC*. pCSMN24 was transferred to *Anabaena* by conjugation. Clones resistant to Sm and
155 Sp were selected and their genetic structure was verified by PCR with primer pairs alr4781-3/gfp-5 and

alr4781-3/alr4781-4. This strain was named CSMN13 (Fig. S4). To prepare an *Anabaena* strain producing a fusion of the GFP to GlsP, a 482-bp DNA fragment from the 3' region of *glsP* (*all0261*) was amplified using *Anabaena* DNA as template and primers all0261-6 and all0261-5. The PCR product, a SacI-NheI fragment, was inserted together with NheI-SalI digested *gfp-mut2* into SacI-XhoI-digested pRL277 (37), producing pCSMN25, which bears a fusion of the *all0261* coding sequence to the *gfp-mut2* gene. This construct was verified by sequencing and transferred to *Anabaena* by conjugation. Clones resistant to Sm and Sp were isolated, and integration of the *glsP-gfp* construct was verified by PCR using primer pairs all0261-4/gfp-5 and all0261-3/all0261-4. This strain was named CSMN15 (Fig. S4).

To study the effect of inactivation of transporter genes on the localization of SepJ-GFP, Nm^R plasmid pCSVT22 bearing *sepJ-gfp* (13) was transferred to strains DR3912a (*alr4781*::C.S3) and DR3915 (*all0261*::C.S3) by conjugation. Similarly, the Sm^RSp^R plasmid pCSAM137 bearing *sepJ-gfp* (12) was transferred to FQ163 (*hepP*::Tn5-1063; 36). The genetic structure of selected clones bearing *sepJ-gfp* fusions was studied by PCR with DNA from those clones and primer pair alr2338-3/gfp-5 to test recombination in the correct genomic location (*sepJ*). We also verified the mutant background in the exconjugants using the following primer pairs: for *alr4781*, alr4781-3/alr4781-4; for *all0261*, all0261-3/all0261-4; and for *hepP*, all1711-3/all1711-4 (Fig. S5). Clones bearing the *sepJ-gfp* fusion were named strain CSMN9 (*alr4781* background), CSMN10 (*all0261* background) and CSMN16 (*hepP* background).

RT-qPCR. RNA was isolated as described (36) from 50 to 100 ml of shaken *Anabaena* cultures. RNA was treated with Ambion® TURBO DNA-free™ DNase according to the manufacturer's protocol. Three independent RNA samples were analyzed from each strain (the wild type and the complemented *glsC* and *glsP* strains) and three technical replicas were carried out for each sample. RNA (200 ng) was reverse-transcribed using QuantiTect® Reverse Transcription Kit (Qiagen) with random primers as indicated by standard protocols of the manufacturer. Quantitative real-time PCR was performed on an *iCycler iQ Real Time PCR Detection System* equipped with the software *iCycler iQ* v 3.0 from BioRad. PCR amplification was performed in a 20-µl reaction mix according to standard protocols of SensiFAST™ SYBR and Fluorescein Kit (Bioline). The Q-PCR conditions were as follows: 1 cycle at 95

ºC for 2 min, 30 cycles of: 95 ºC for 15 s, 67.5 ºC for 20 s and 72 ºC for 30 s. PCR products were checked by a single-peak melting curve. The threshold cycle (Ct) of each gene was determined and normalized to those of reference genes *ispD* (*all5167*) and *dxs* (*alr0599*), to obtain ΔCt values from each sample. Relative gene expression was calculated using the $2^{-\Delta\Delta Ct}$ method (39), and the data presented correspond to the average of data obtained with each reference gene. The following primer pairs were used: all0261-11/all0261-12, alr4781-9/alr4781-10, all5167-1/all5167-2 and alr0599-1/alr0599-2 (Table S1).

Uptake of esculin. *Anabaena* strains grown in BG11 medium—with antibiotics for the mutants—were harvested by centrifugation, washed three times with BG11 or $BG11_0$ medium without antibiotics and incubated for 18 h in the same medium under culture conditions. Cells were harvested, washed and resuspended in the corresponding growth medium supplemented with 10 mM HEPES-NaOH buffer (pH 7, unless indicated otherwise), and 1 mM of the indicated sugar in the experiment described in Fig. 3. Assays of uptake were started by addition of esculin hydrate (Sigma-Aldrich) at 100 µM, and suspensions were incubated at 30ºC in the light (~170 µmol photons m^{-2} s^{-1}) for up to 70 min. One-ml samples were withdrawn and filtered. Cells on the filters were washed with 10 mM HEPES-NaOH buffer of the same pH used in the assay and were resuspended in 2 ml of 10 mM HEPES-NaOH buffer (pH 7). Fluorescence of the resulting cell suspension was measured in a Varian Cary Eclipse Fluorescence Spectrophotometer (excitation 360 ± 10 nm; emission 462 ± 10 nm). Esculin solutions in the same buffer (pH 7) were used as standards. Significance in the differences of uptake between strains (as well as in other parameters investigated in this work) was assessed by unpaired Student's *t* tests, assuming a normal distribution of the data. Data sets with values of $P < 0.05$ are considered significant.

Growth curves and nitrogenase activity. The growth rate constant ($\mu=[\ln 2]/t_d$, where t_d is the doubling time) was calculated from the increase in $OD_{750\ nm}$ of shaken liquid cultures. Cultures were inoculated with an amount of cells giving an $OD_{750\ nm}$ of about 0.05 (light path, 1 cm) and grew logarithmically until reaching an $OD_{750\ nm}$ of about 0.8-0.9. The suspensions of filaments were carefully homogenized with a pipette before taking the samples.

For determination of nitrogenase activity, filaments grown in BG11 medium were harvested, washed with $BG11_0$ medium, and resuspended in $BG11_0$ medium. After 48 h of incubation under growth conditions, the filaments were used in acetylene reduction assays performed under oxic or anoxic conditions at 30ºC in the light (ca. 150 µmol photons m^{-2} s^{-1}). For these assays, the cell suspensions (2 ml, ca. 10 µg Chl ml^{-1}) were placed in flasks sealed with rubber stoppers (total volume, 12 to 14 ml). For the anoxic assays, the cell suspensions were supplemented with 10 µM DCMU, bubbled thoroughly with argon for 3 min, and incubated for 60 min under assay conditions before starting the reaction. Production of ethylene, determined by gas chromatography in 1-ml samples from the gas phase, was followed for up to three hours after starting the reaction by addition of acetylene (2 ml).

Light, confocal and fluorescence microscopy. Cultures were routinely observed by light microscopy. To stain the polysaccharide layer of heterocysts, cell suspensions were mixed (1:2) with a filtered 1% (w/v) Alcian Blue (Sigma) solution.

For visualization by confocal microscopy of filaments of strains producing genetic fusions to GFP, small blocks of agar-solidified BG11 or $BG11_0$ medium bearing the filaments were excised and placed in a sample holder with a glass cover slip on top. GFP fluorescence was visualized using a Leica HCX PLAN-APO 63X 1.4 NA oil immersion objective attached to a Leica TCS SP2 confocal laser-scanning microscope. GFP was excited using 488-nm irradiation from an argon ion laser. Fluorescent emission was monitored by collection across windows of 498-541 nm (GFP imaging) and 630-700 nm (cyanobacterial autofluorescence). GFP fluorescence intensity was analyzed using ImageJ 1.45s software. To determine the relative fluorescence intensity in different cell zones, integrated density was recorded in squares of 0.2 to 0.8 μm^2. About 80 to 190 measurements were made for each of the lateral walls and septal areas of vegetative cells from BG11 or $BG11_0$ medium, and 50 to 60 measurements were made for lateral walls of heterocysts. We could not accurately quantify GFP fluorescence from heterocyst-vegetative cell septa, which are thinner than the septa between vegetative cells. Because fluorescence did not follow a normal distribution, data are presented as median (*m*) and interquartile ranges (IQR) (40).

For fluorescence microscopy, filaments of cells were imaged using a Leica DM6000B

233 fluorescence microscope and an ORCA-ER camera (Hamamatsu). GFP fluorescence was monitored using
234 a FITC L5 filter (excitation BP 480/40, emission BP 527/30) and red autofluorescence was monitored
235 using a Texas Red TX2 filter (excitation BP 560/40, emission BP 645/75).

236 **Immunolocalization of SepJ.** Cells from 1.5 ml of liquid cultures were collected by
237 centrifugation, placed atop a poly-L-lysine pre-coated microscope slide and covered with a 45-µm pore-
238 size Millipore filter. The filter was removed and the slide was let to dry at room temperature and, then,
239 immersed in 70% ethanol at -20ºC for 30 min and dried 15 min at room temperature. The cells were
240 washed twice (2 min each time, room temperature) by covering the slide with PBS-T (PBS supplemented
241 with 0.05% Tween-20). Subsequently, the slides were treated with a blocking buffer (5% milk powder in
242 PBS-T) for 15 min. Cells on the slides were then incubated for 90 min with anti-SepJ-CC antibodies (17)
243 diluted in blocking buffer 1:250, washed three times with PBS-T, incubated 45 min in the dark with anti-
244 rabbit antibody conjugated to fluorescein isothiocyanate (FITC) (Sigma, 1:500 dilution in PBS-T) and
245 washed three times with PBS-T. After dried, several drops of FluorSave (Calbiochem) were added atop,
246 covered with a coverslip and sealed with nail lacquer. Fluorescence was monitored as above, and images
247 were analyzed with ImageJ software (http://imagej.nih.gov/ij).

248 **Visualization of nanopores by electron microscopy.** The murein sacculi (which are made of
249 peptidoglycan) were isolated from filaments grown in BG11 medium and analyzed as described
250 previously (18, 19). The purified sacculi were deposited on formvar/carbon film coated copper grids, and
251 stained with 1% (w/v) uranyl acetate. All the samples were examined with a ZEISS LIBRA 120 PLUS
252 electron microscope at 120 kV.

253 **FRAP (fluorescence recovery after photobleaching) analysis.** For assays of intercellular transfer
254 of esculin, filaments were harvested, resuspended in 500 µl of fresh growth medium, mixed with 15 µl of
255 saturated (~5 mM) aqueous esculin hydrate solution and incubated for 1 hour in the dark with gentle
256 shaking at 30°C, then washed three times with growth medium, followed by dark incubation for 15 min in
257 1 ml medium at 30°C with gentle shaking. Cells were then washed, spotted onto a BG11 or $BG11_0$ agar
258 plate (1% w/v), and excess medium was removed. Small blocks of agar with cells adsorbed on the surface

were placed in a custom-built temperature-controlled sample holder under a glass cover slip at 30°C except when indicated otherwise. Cells were visualized with a laser-scanning confocal microscope (Leica TCS SP5) using a Leica HCX Plan Apo 63X NA 1.4 oil-immersion objective. Fluorescence was excited at 355 nm, with detection of esculin at 443-490 nm and detection of Chl at 670-720 nm. High-resolution imaging used a 6x line-average with an optical section of ~0.7 µm. FRAP measurements were without line averaging and with a wide pinhole giving an optical section of ~4 µm. After capturing a pre-bleach image, the fluorescence of a defined region of interest was bleached out by scanning this region at ~6x higher laser intensity, and recovery was then recorded in a sequence of full-frame images.

For calcein and 5-CF transfer assays, calcein and 5-CF staining and FRAP analysis were performed as previously reported (7, 14). Cell suspensions were spotted onto agar and placed in a custom-built temperature-controlled sample holder with a glass cover slip on top. All measurements were carried out at 30°C. For both calcein and 5-CF, cells were imaged with a Leica HCX PLAN-APO 63X 1.4 NA oil immersion objective attached to a Leica TCS SP5 confocal laser-scanning microscope as previously described for calcein (7) with a 488-nm line argon laser as the excitation source. Fluorescent emission was monitored by collection across windows of 500-520 nm or 500-527 nm in different experiments and a 150-µm pinhole. After an initial image was recorded, the bleach was carried out by an automated FRAP routine which switched the microscope to X-scanning mode, increased the laser intensity by a factor of 10, and scanned a line across one cell for 0.137 s before reducing the laser intensity, switching back to XY-imaging mode and recording a sequence of images typically at 1 s intervals.

For FRAP data analysis, we quantified kinetics of transfer of the fluorescent tracer either (i) to a terminal cell (with one cell junction) or (ii) a cell somewhere in the middle of a filament (i.e., with two cell junctions). For (i), the recovery rate constant R was calculated from the formula $C_B = C_0 + C_R (1 - e^{-Rt})$, where C_B is fluorescence in the bleached cell, C_0 is fluorescence immediately after the bleach and tending towards $(C_0 + C_R)$ after fluorescence recovery, t is time and R is the recovery rate constant due to transfer of the tracer from one neighbor cell (14). For (ii), the formula $C_B = C_0 + C_R (1 - e^{-2Rt})$ was used. Development of equations for FRAP analysis is described in Supporting information (Text S1).

Bacterial Adenylate Cyclase Two-Hybrid (BACTH) strain construction and assays. The possible interaction of the different glucoside transporters with SepJ was tested using BACTH. For this analysis, all tested genes were amplified using *Anabaena* DNA as template. The following primers were used: alr4781-7 and alr4781-8 to amplify *glsC*; all0261-7 and all0261-8 to amplify *glsP*; and all1711-9 and all1711-10 to amplify *hepP*. The PCR products were cloned in vector pSpark I, transformed into *E. coli* DH5α and sequenced. Inserts with the correct sequence were transferred as XbaI- and KpnI-digested fragments to pUT18, pUT18C, pKNT25 and pKT25 producing fusions to the 5' and 3' ends of the genes encoding the adenylate cyclase T18 and T25 fragments, respectively. The resulting plasmids were transformed into *E. coli* XL1-Blue to amplify the plasmids. Fusions of the *sepJ* gene to the 5' end of T18 or T25 were as previously described (15). Isolated plasmids were co-transformed into BTH101 (*cya-99*). Transformants were plated onto LB medium containing selective antibiotics and 1% glucose. Efficiencies of interactions between different hybrid proteins were quantified by measurement of β-galactosidase activity in cells from liquid cultures.

To determine β-galactosidase activity, bacteria were grown in LB medium in the presence of 0.5 mM IPTG and appropriate antibiotics at 30ºC for 16 h. Before the assays, cultures were diluted 1:5 into buffer Z (60 mM Na_2HPO_4, 40 mM NaH_2PO_4, 10 mM KCl and 1 mM $MgSO_4$). To permeabilize cells, 30 µl of toluene and 35 µl of a 0.1% SDS solution were added to 2.5 ml of bacterial suspension. The tubes were vortexed for 10 s and incubated with shaking at 37ºC for 30 min for evaporation of toluene. For the enzymatic reaction, 875 µl of permeabilized cells were added to buffer Z supplemented with β-mercaptoethanol (25 mM final concentration), to a final volume of 3.375 ml. The tubes were incubated at 30ºC in a water bath for at least 5 min. The reaction was started by adding 875 µl of 0.4 mg ml^{-1} *o*-nitrophenol-β-galactoside (ONPG) in buffer Z. Samples of 1 ml, taken at different times (up to 12 min), were added to 0.5 ml of 1 M Na_2CO_3 to stop the reaction. $A_{420\ nm}$ was recorded, and the amount of *o*-nitrophenol produced was calculated using an extinction coefficient $\varepsilon_{420\ nm}$=4.5 mM^{-1} cm^{-1} and referred to the amount of total protein, determined by a modified Lowry procedure.

310

311 **RESULTS**

312 **Esculin uptake through α-glucoside transporters.** We have previously shown that esculin can be taken
313 up by *Anabaena* filaments grown in BG11 medium (containing nitrate as the nitrogen source) or grown in
314 BG11 medium and incubated for 18 hours in $BG11_0$ medium (lacking any source of combined nitrogen),
315 and that uptake is linear for at least 70 min and takes place at higher levels in the filaments incubated in
316 $BG11_0$ medium (18). To understand better the process of esculin uptake, we determined the dependence
317 of esculin uptake on esculin concentration. Esculin uptake was faster in cells that had been incubated in
318 the absence of nitrate, compared to nitrate-grown cultures, with V_{max} values of about 0.31 and 0.57 nmol
319 $(mg\ Chl)^{-1}\ min^{-1}$ for BG11-grown filaments and filaments incubated in $BG11_0$ medium, respectively (Fig.
320 1). Esculin concentrations giving half-maximal uptake rates (K_s) were 150 and 119 µM in BG11 and
321 $BG11_0$, respectively. Because a concentration somewhat lower than the K_s would permit observation of
322 effects such as competitive or non-competitive inhibition, we have used 100 µM esculin as a standard
323 concentration in our uptake assays.

324 The pH-dependence of uptake of esculin was investigated. As shown in Fig. 2, the rate of uptake
325 was higher at pH 7 than at lower or higher pH values, and was in every case higher in filaments incubated
326 in $BG11_0$ medium than in filaments from BG11 medium. The difference in the rate of uptake between
327 filaments from $BG11_0$ and BG11 media decreased as the pH of the assay buffer was increased, suggesting
328 that a H^+-dependent transporter is induced in filaments incubated in $BG11_0$ medium.

329 Esculin has been used to test the activity of some higher plant sucrose transporters (41) and,
330 consistent with the possibility of uptake through sucrose transporter(s), inhibition of uptake of esculin by
331 sucrose has been observed in *Anabaena* (18). To characterize further the transporters involved, we tested
332 whether uptake of esculin would be inhibited by various monosaccharides (glucose, fructose, and
333 galactose) and disaccharides (sucrose, maltose, trehalose, and lactose). The results in Fig. 3 show that, in
334 BG11-grown filaments, uptake of esculin is inhibited mainly by sucrose and, to a lesser extent, by

maltose. Other sugars tested appear to have stimulated uptake of esculin. In filaments that were incubated in $BG11_0$ medium, inhibition of uptake by sucrose and maltose was again evident. Our results suggest that although esculin is a β-glucoside, its uptake is inhibited mainly by some α-glucosides, sucrose (glucose 1α —> 2 fructose) and maltose (glucose 1α —>4 glucose), whereas neither lactose (a β-galactoside; galactose 1β—>4 glucose) nor trehalose (a different α-glucoside; glucose 1α—>1α glucose) inhibits uptake of esculin.

Identification of three transporters mediating esculin uptake. Two genes, Ava_2050 and Ava_2748, that encode possible components of ABC uptake transporters for disaccharides or oligosaccharides are induced in the heterocysts of *Anabaena variabilis* ATCC 29413 (42). BLAST analysis with the genomic sequence of *Anabaena* (43) identified Alr4781 and All0261, with 97% and 99% amino acid identity, respectively, as the products of the *Anabaena* orthologs of those *A. variabilis* genes. Among characterized proteins included in the Transporter Classification Database (TCDB; http://www.tcdb.org), Alr4781 is most similar (45.4% identity, 59.6% similarity; expect, 3.2×10^{-111}) to MalK1, an ATP-binding subunit shared by the glucose/mannose (TCDB no. 3.A.1.1.24) and the trehalose/maltose/sucrose/palatinose (TCDB no. 3.A.1.1.25) transporters from *Thermus thermophilus*, and All0261 is most similar (36.4% identity, 58.9% similarity; expect, 3.3×10^{-51}) to the AraQ permease component of the arabinosaccharide transporter AraNPQ-MsmX from *Bacillus subtilis* (TCDB no. 3.A.1.1.34). We denote *alr4781* as *glsC* and *all0261* as *glsP* (*gls* standing for glucoside). Neither *glsC* nor *glsP* is clustered together with other ABC transporter-encoding genes in the *Anabaena* genome. To test whether the transporters encoded by these *Anabaena* genes can be involved in uptake of esculin, *glsC* was inactivated by insertion of gene-cassette C.S3 (44), resulting in *Anabaena* strains that bear the DR3912a mutation (Fig. S1), and *glsP* was inactivated by insertion of C.S3, resulting in *Anabaena* strains that bear the DR3915 mutation, or of C.CE1 (44), resulting in *Anabaena* strains that bear the DR3985a mutation (Fig. S1). BG11-grown filaments of the *glsC* and *glsP* mutants showed esculin uptake activities that were 49% and 59% of the wild-type activity, respectively (Table 1), and filaments of the *glsC* and *glsP* mutants

that had been incubated in $BG11_0$ medium showed 74% and 73% of the wild-type activity, respectively. Thus, the products of both genes contribute to esculin uptake by *Anabaena* in medium containing nitrate (BG11) and after incubation in medium lacking combined nitrogen ($BG11_0$).

ABC uptake transporters typically comprise one periplasmic solute-binding protein, two integral membrane proteins (transmembrane domains or permeases) and two nucleotide-binding domains that hydrolyze ATP in the cytoplasm (45). If the GlsC ATP-binding subunit and the GlsP permease belong to the same ABC transporter, we would expect that mutation of the two genes would not increase the effect on the uptake of esculin over that of the single mutations. If, on the other hand, GlsC and GlsP belong to two different transporters, we would expect an additive effect of the mutations. A double *glsC glsP* mutant, i.e., an *Anabaena* strain bearing the DR3912a and DR3985a mutations (Fig. S1), showed 25% of the wild-type activity of esculin uptake in BG11-grown filaments and 50% in filaments incubated in $BG11_0$ medium (Table 1), percentages that represent decreased values compared to the effects of the single mutations (49% and 59% for BG11 and 74% and 73% for $BG11_0$). These results suggest that GlsC and GlsP are components of different ABC transporters that can mediate esculin uptake. Notably, a significant uptake activity remains in the double mutant, especially in filaments that had been incubated in medium lacking combined nitrogen ($BG11_0$).

Genes *all1711* (*hepP*) and *alr3705* encode predicted MFS proteins that would facilitate movement of disaccharides or oligosaccharides across cell membranes. As shown by results with mutant *all1711*::Tn*5*-1063, strain FQ163 (36), HepP may be a glucoside transporter that is involved in production of the heterocyst-specific polysaccharide layer and may also mediate sucrose transport. According to BLAST analysis, Alr3705 is the predicted *Anabaena* genomic product most similar to higher plant sucrose transporters. *alr3705* was mutated by insertion of C.S3-containing plasmid pCSRL49, producing strain CSRL15, and insertion of pCSRL49 was also combined with *all1711*::Tn5-1063 to produce a double mutant, strain CSMN3 (Fig. S3). None of strains FQ163, CSRL15, or CSMN3, when grown in BG11 medium, was significantly affected in uptake of esculin (Student's *t* test *P* values 0.553 to 0.703; Table 1), nor was CSRL15 significantly affected when incubated in $BG11_0$ medium (Table 1). In contrast,

386 filaments of mutants FQ163 and CSMN3 incubated in $BG11_0$ medium showed similarly decreased
387 activities, 69% and 67% of the wild-type activity, respectively (Table 1). These results indicate that HepP,
388 but not Alr3705, contributed to uptake of esculin in filaments deprived of combined nitrogen.

389 In conclusion, two ABC transporters, of which GlsC and GlsP are independent components, are
390 together responsible for about 75% and 50% of uptake of esculin in BG11- and $BG11_0$-filaments,
391 respectively, and HepP is responsible for about 30% of uptake of esculin in $BG11_0$-filaments, when tested
392 at pH 7. Other transporters should therefore contribute to uptake of esculin in both BG11 and $BG11_0$
393 media.

394 **Subcellular localization of GlsC and GlsP.** To understand better the role of the transporters
395 identified in this work in the physiology of *Anabaena*, we investigated their subcellular localization. The
396 localization of HepP in the cytoplasmic membrane of both vegetative cells and heterocysts has been
397 described previously (36). To study the subcellular localization of GlsC and GlsP, strains producing
398 GlsC-GFP and GlsP-GFP fusion proteins were constructed. As a putative nucleotide-binding domain of
399 an ABC transporter, GlsC is expected to reside in the cytoplasmic face of the cytoplasmic membrane.
400 GlsP is a predicted integral membrane protein that bears six putative transmembrane segments with both
401 the N- and C-termini in the cytoplasm. Because the GFP protein folds efficiently in the cytoplasm (46),
402 the *gfp-mut2* gene was added to the 3' end of the *glsC* and *glsP* genes, and the corresponding constructs
403 were transferred to *Anabaena* (Fig. S4). Visualization of filaments of the corresponding strains, CSMN13
404 (*glsC-gfp*) and CSMN15 (*glsP-gfp*), incubated in BG11 or $BG11_0$ medium, showed a relatively low GFP
405 signal that was spread through the periphery of the cells including the septal regions, where the signal was
406 increased (Fig. 4). Quantification of GFP fluorescence was performed as described in Materials and
407 Methods and is summarized in Fig. S6. The data show that fluorescence was roughly two-fold higher in
408 the septa than in lateral areas for both GlsC-GFP and GlsP-GFP in cells grown in BG11 medium as well
409 as in cells incubated in $BG11_0$ medium, indicating that the increased fluorescence from the septa likely
410 corresponds to the combination of the fluorescence from the adjacent cytoplasmic membranes.
411 Nonetheless, somewhat larger GFP fluorescence was observed in septal areas of cells grown in BG11

412 medium than of cells incubated in $BG11_0$ medium. In filaments incubated in $BG11_0$ medium, the GFP
413 signal was present at similar levels in heterocysts and vegetative cells. These results indicate that GlsC
414 and GlsP are located throughout the cytoplasmic membrane of both vegetative cells and heterocysts. Our
415 results also indicate that levels of GlsC-GFP or GlsP-GFP are generally similar in cells incubated in
416 BG11 and $BG11_0$ media (Fig. S6).

417 **Fox phenotype of the *glsC* and *glsP* mutants.** The Fox^- phenotype denotes inability to grow
418 fixing N_2 under oxic conditions, and it is frequently associated with malformation of the heterocyst
419 envelope, as in the case of the *hepP* mutant (36). The growth phenotype was here investigated for the
420 *glsC* and *glsP* mutants. On solid medium, the *glsC* and *glsP* single mutants and the *glsC glsP* double
421 mutant could grow using nitrate as the nitrogen source or fixing N_2, but the *glsP* mutant showed poorer
422 diazotrophic growth than the wild type and the *glsC* and *glsC glsP* mutants showed poorer growth in both
423 media (Fig. 5). To determine growth rate constants, growth tests were carried out in liquid medium. In the
424 presence of nitrate (BG11 medium) the growth rate of the single mutants was identical to that of the wild
425 type, whereas the growth rate of the double mutant was 75% that of the wild type (Table 2). In the
426 absence of combined nitrogen ($BG11_0$ medium), the growth rate of the three mutants was lower than that
427 of the wild type, being especially low in the case of the double mutant (Table 2). Thus, the *glsC*, *glsP* and
428 *glsC glsP* mutants cannot grow normally fixing N_2 under oxic conditions, and therefore show, at best, a
429 weak Fox^+ phenotype. The phenotype of diminished growth of the single mutants could be complemented
430 by introducing in the corresponding mutant a replicative plasmid bearing the wild-type gene, *glsC* or
431 *glsP*, but, tested on solid medium, complementation was incomplete (Fig. S2). To investigate whether
432 incomplete complementation could result from insufficient expression of the genes in the complemented
433 strains, RT-qPCR analysis was performed as described in Materials and Methods. Rather than low
434 expression, this analysis indicated 6-fold and 11-fold higher expression of the *glsC* and *glsP* genes,
435 respectively, in the complemented mutants than in the wild type. It is possible therefore that
436 overexpression of these genes is deleterious for *Anabaena*.

Production of heterocysts and nitrogenase activity were determined in filaments grown in BG11 medium and incubated for 48 hours in $BG11_0$ medium. The *glsC*, *glsP* and *glsC glsP* mutants showed, respectively, about 60%, 85% and 24% the number of heterocysts observed in the wild type (Table 2). Under oxic conditions, nitrogenase activity was about 10% of the wild-type activity in the two single mutants, and about 6.5% in the double mutant (Table 2). Thus, the heterocysts produced in the mutants exhibited low nitrogenase activity. Assay under anoxic conditions showed little or no increase in activity, in contrast to what is normally observed in mutants that bear a defect in the heterocyst envelope (see, for instance, ref. 36). The heterocyst envelope-specific polysaccharide layer can be stained with Alcian Blue, a stain useful to detect bacterial polysaccharides (47). Microscopic inspection of filaments of the *glsC glsP* double mutant stained with Alcian Blue showed the presence of stained heterocysts, indicating the existence of a polysaccharide layer in the double mutant (Fig. 6). Microscopic inspection also showed that the filaments of the double mutant were very short (Fig. 6). Inspection of cultures of the three mutants showed the presence of short filaments in the *glsC glsP* double mutant in both BG11 and $BG11_0$ media, but filament fragmentation was strongest in $BG11_0$ medium (Fig. S7). Such short filaments were not observed in the *glsC* or *glsP* single mutants. Thus, the phenotypic alterations were stronger in the *glsC glsP* double mutant than in the *glsC* or *glsP* single mutants, which is consistent with independent action of the GlsC and GlsP proteins as concluded above from the esculin uptake data.

Intercellular exchange of fluorescent markers. Because the *glsC*, *glsP*, and *hepP* mutants are impaired in glucoside transport and diazotrophic growth, the proteins encoded by these genes could influence somehow intercellular transfer of sucrose. We therefore tested intercellular exchange of esculin in the *glsC*, *glsP*, and *hepP* mutants by means of FRAP analysis. The results of these tests were analyzed to determine the recovery constant (*R*) of fluorescence in the cells in which esculin had been bleached (see Materials and Methods and Text S1). To attain adequate labeling of esculin to carry out the FRAP analysis, filaments were incubated for one hour with 150 μM esculin. Transfer of esculin between vegetative cells of BG11-grown filaments was decreased in a limited way (by about 22%) in the *glsC*

462 mutant, although not in the *glsP* mutant (Table 3). However, the effect was larger in the *glsC glsP* double
463 mutant (about 33% inhibition). In the *hepP* mutant, esculin transfer was 43% lower than in the wild type.
464 In filaments of the wild type that had been incubated for 48 h in $BG11_0$ medium, esculin transfer
465 between vegetative cells was similar to transfer between BG11-grown vegetative cells, but transfer from
466 vegetative cells to heterocysts was decreased to about 38% the value between vegetative cells (Table 3).
467 These results are consistent with previously reported data (18). In the mutants, esculin transfer was lower
468 in the $BG11_0$-incubated than in the BG11-grown vegetative cells, and it was especially decreased in the
469 *glsC* mutant (Table 3). In contrast, esculin transfer from vegetative cells to heterocysts was increased in
470 all the mutants as compared to the wild type, and this increase was particularly significant in the *hepP*
471 mutant. In summary, esculin transfer was impaired between vegetative cells of heterocyst-containing
472 filaments, but not from vegetative cells to heterocysts.
473 To assess how specific the effect on intercellular transfer could be, transfer of calcein and 5-CF
474 between nitrate-grown vegetative cells was also tested in the mutants. Calcein transfer was significantly
475 impaired in the three single mutants, and it was lowest (21% of the wild-type activity) in the *glsC glsP*
476 double mutant (Table 4). Transfer of 5-CF was also significantly impaired in the *glsC* and *glsP* mutants,
477 although the effect of the mutations was lower in this case than on calcein transfer, and it was not
478 impaired in the *hepP* mutant. These studies showed that GlsC, GlsP, and HepP are required for normal
479 intercellular molecular exchange in *Anabaena*, but this requirement is more evident when the exchange is
480 tested with calcein than with 5-CF or, as shown above, esculin (compare BG11-grown filaments).
481 **SepJ localization and nanopores in the *glsC*, *glsP* and *hepP* mutants.** The fragmentation of
482 filaments observed in the *glsC glsP* double mutant and the effect of the mutation of the glucoside
483 transporters on calcein exchange described above are reminiscent of effects of inactivation of *sepJ* in
484 *Anabaena* (12, 18). We therefore investigated the effect of the inactivation of *glsC*, *glsP* and *hepP* on the
485 subcellular localization of SepJ. For this investigation, plasmids bearing a *sepJ-gfp* fusion gene were
486 transferred to mutants of those genes producing strains CSMN9 (*glsC sepJ-gfp*), CSMN10 (*glsP sepJ-*
487 *gfp*), and CSMN16 (*hepP sepJ-gfp*) (for PCR analysis of the genomic structure of each strain, see Fig.

S5). Confocal microscopic inspection of filaments of strains producing SepJ-GFP showed that, whereas the *glsP* and *hepP* mutations did not impair SepJ-GFP localization at the intercellular septa, the *glsC* mutation had a strong effect on localization (Fig. 7; for SepJ-GFP localization in four independent clones inspected by fluorescence microscopy, see Fig. S8). In the *glsC sepJ-gfp* strain, spots of GFP were only sporadically observed in the center of the septa, and the GFP signal was frequently found throughout the periphery of the cells including the intercellular septa. Thus, GlsC, but not GlsP or HepP, appears necessary for proper subcellular localization of SepJ.

To corroborate delocalization of SepJ as a result of inactivation of *glsC*, immunolocalization of SepJ was performed using antibodies raised against its coiled-coil domain (17). The antibodies localized SepJ at the cell poles of *Anabaena* (Fig. 8), as previously described (15). In the *glsC* mutant, the signal was largely delocalized, being observed at the cell poles only sporadically. In the complemented strain *glsC-C* (DR3912a [pCSMN22]), SepJ was observed clearly at the cell poles (Fig. 8). These results are fully consistent with the observation that the SepJ-GFP fusion protein shows delocalization of SepJ as the result of inactivation of *glsC* (Figs. 7 and S8).

Because SepJ is necessary for *Anabaena* to make a normal number of septal peptidoglycan nanopores (18), the number of nanopores was counted in septal peptidoglycan disks observed in murein sacculi isolated from the wild type and the *glsC*, *glsP* and *hepP* mutants (Fig. 9). Whereas the *glsP* and *hepP* mutants contained a number of nanopores per septum similar to that of the wild type, the septa of the *glsC* mutant contained about 48% of the nanopores found in the wild-type septa.

Protein-protein interactions. The results in the previous section, showing that GlsC is necessary for proper localization of SepJ and formation of septal peptidoglycan nanopores, provides a rationale for understanding the effect of inactivation of *glsC* on the intercellular transfer of calcein, but no effect of inactivation of *glsP* or *hepP* was found. We then studied possible protein-protein interactions involving the glucoside transporters and SepJ using the BACTH assay, in which adenylate cyclase activity is reconstituted from two fragments, T25 and T18, of an adenylate cyclase from *Bordetella pertussis* brought together by interacting proteins fused to each of those fragments (48). Reconstituted adenylate

514 cyclase in *E. coli* produces cAMP that promotes induction of *lacZ* encoding β-galactosidase. We have
515 previously shown that SepJ-T25 and SepJ-T18 fusions (where the order of protein names denotes N-
516 terminal to C-terminal orientation) are functional in SepJ self-interactions that produce high β-
517 galactosidase activity (15, 16). As is the case for GlsP, HepP is a predicted integral membrane protein
518 with both the N- and C-termini in the cytoplasm (36). Because of possible copy number or steric
519 hindrance problems (49, 50), here we tested possible interactions of SepJ-T25 and SepJ-T18 with both N-
520 terminal and C-terminal fusions to T18 and T25, respectively, of each of the glucoside transporter
521 components investigated in this work, GlsC, GlsP and HepP. The negative control in this analysis is an *E.*
522 *coli* strain carrying plasmids that produce non-fused T25 and T18 fragments, and additional negative
523 controls producing non-fused T25 or T18 and some of the tested fusions were carried out. None of these
524 controls produced β-galactosidase activity significantly different from that of the T25/T18 control (Table
525 5). Combinations of protein fusions involving SepJ that produced β-galactosidase activity significantly
526 higher than the controls included SepJ-T25/SepJ-T18 (positive control), SepJ-T25/T18-HepP, SepJ-
527 T18/T25-HepP and SepJ-T18/T25-GlsP, but no fusion involving GlsC. These results suggest significant
528 interactions between SepJ and GlsP and, more strongly, between SepJ and HepP. On the other hand,
529 significant interactions were also observed between HepP and GlsP. Finally, HepP self-interactions and
530 GlsC self-interactions were also observed suggesting that HepP and GlsC can form homo-oligomers.
531
532 **DISCUSSION**
533 **Glucoside transporters.** Esculin has been successfully used as a fluorescent analog of sucrose to study
534 intercellular molecular exchange in the filaments of *Anabaena* by means of FRAP analysis (18). This
535 analysis requires esculin to be taken up by the cells in the filament, and we have now identified three
536 genes, *glsC*, *glsP* and *hepP*, that encode components of transporters that mediate esculin uptake in
537 *Anabaena*. The *glsC* (*alr4781*) gene encodes an ATP-binding subunit of an ABC transporter, and the *glsP*
538 (*all0261*) gene encodes an integral membrane (permease) subunit of a different ABC transporter. These

539 genes were investigated because they are the possible *Anabaena* orthologs of genes highly expressed in
540 the heterocysts of a closely related cyanobacterium, *A. variabilis* (42). In *Anabaena*, because the effect of
541 inactivating *glsC* and *glsP* is evident in filaments grown in the presence of nitrate (Table 1), GlsC and
542 GlsP appear to be active in vegetative cells. Additionally, as observed with GFP fusions, GlsC and GlsP
543 are present in heterocysts as well as in vegetative cells (Fig. 4, Fig. S6). In transcriptomic analysis of
544 *Anabaena*, these genes appear to have low expression, and their expression is not affected by nitrogen
545 deprivation (51). According to the results of inhibition of uptake of esculin by sugars (Fig. 3), the natural
546 substrate of these transporters can be sucrose or an α-glucoside. Sucrose uptake by vegetative cells of
547 *Anabaena* has previously been reported (52), and sucrose transporters that can also transport maltose are
548 frequently found in plants (53). The *Anabaena* glucoside transporters could have a role in the recovery of
549 glucosides from extracellular polysaccharides produced under certain physiological conditions, as has
550 been shown to occur in cyanobacterial mats (54). Consistently, biomass of the *glsC* and *glsP* mutants in
551 old BG11 plates is shiny (not shown), which may be indicative of exo-polysaccharide accumulation (36).
552 It is of interest to note also that, although *Anabaena* has been considered an obligatory photoautotroph
553 (28), recent data suggests that it can grow using fructose, albeit this sugar has to be provided at a high
554 concentration unless *Anabaena* is engineered to express a fructose transporter (27, 55). On the other hand,
555 trehalose, lactose, glucose, fructose, and galactose could stimulate esculin uptake (Fig. 3), suggesting that
556 *Anabaena* can use these sugars to support physiological activities such as active transport. As noted
557 earlier, the *Anabaena* genome bears several genes putatively encoding sugar transporters (27), some of
558 which could be involved in the uptake of those sugars.

559 The third gene that encodes an esculin transporter is *hepP* (*all1711*), which encodes an MFS
560 protein that is also necessary for production of the heterocyst-specific polysaccharide layer (36). We have
561 previously shown that HepP is present at higher levels in developing heterocysts (proheterocysts) and
562 heterocysts than in vegetative cells, and that HepP could possibly mediate sucrose uptake specifically in
563 (pro)heterocysts (36). Because the contribution of HepP to uptake of esculin is evident only in filaments
564 that had been incubated in the absence of combined nitrogen, and because uptake of esculin in these

565 filaments is inhibited by sucrose, HepP may be involved in uptake of sucrose/esculin by (pro)heterocysts.
566 MFS proteins including sucrose transporters frequently act as secondary transporters that mediate symport
567 with protons (56). Uptake of esculin that is associated with incubation in $BG11_0$ medium less uptake in
568 BG11 medium decreases with increasing pH beyond pH 6 (Fig. 2). This observation suggests that a H^+-
569 dependent transporter is induced in filaments incubated in $BG11_0$ medium. Because HepP contributes to
570 esculin uptake associated with incubation in $BG11_0$ medium, our results are consistent with the idea that
571 HepP may be a sucrose-H^+ or α-glucoside-H^+ symporter.

572 **Glucoside transporter mutant phenotypes.** Inactivation of *hepP* leads to a Fox^- phenotype that
573 has been described in detail (36). We have found that the *glsC* and *glsP* mutants exhibit a weak Fox^+
574 phenotype: they grow slowly without a source of combined nitrogen under oxic conditions and express
575 low levels of nitrogenase activity (Table 2). Combination in the same strain of the two mutations, *glsC*
576 and *glsP*, resulted in a greater impairment of diazotrophic growth, very low nitrogenase activity and a low
577 percentage of heterocysts. Nonetheless, these heterocysts bore an envelope polysaccharide layer (Fig. 6)
578 and their nitrogenase activity was not substantially increased in anoxic assays, suggesting that they do not
579 have a cell envelope problem. To explore the possibility of a limited sucrose supply to the heterocysts, we
580 investigated whether the *glsC* and *glsP* mutations might affect intercellular molecular exchange tested
581 with the fluorescent sucrose analog esculin. We have observed that the transfer of esculin in filaments of
582 strains mutated in *glsC*, *glsP* or *hepP* is impaired between vegetative cells, but not from vegetative cells
583 to heterocysts (Table 3). Impairment of sucrose transfer between vegetative cells might eventually limit
584 sucrose supply to heterocysts, and a low supply of reductant would explain the low nitrogenase activities
585 detected in *glsC*, *glsP*, and *glsC glsP* mutants. In the case of the *glsC glsP* double mutant, the small
586 number of vegetative cells in heterocyst-containing filaments, which are short (Figs. 6 and S7), may
587 further limit the supply of reductant for nitrogenase. On the other hand, esculin transfer to heterocysts was
588 substantially increased in the *hepP* mutant (Table 3). At least some sucrose transporters of the MFS
589 family can function bidirectionally (56), and this could be the case for HepP that appears to export

saccharides from the heterocysts (36). The apparently increased transfer of esculin to heterocysts in the *hepP* mutant might therefore reflect increased retention of esculin in the heterocysts of this strain.

Influence of the glucoside transporters on septal junctions. Starting from the observation that the *glsC*, *glsP* and *hepP* mutants characterized in this work are impaired in the transfer of esculin between vegetative cells, we found that intercellular transfer of fluorescent markers is in general affected in these mutants, with the highest effect being observed on the transfer of calcein. A greater effect on transfer of calcein than of 5-CF or esculin is reminiscent of the effect of inactivation of *sepJ* (14, 17, 18). Hence, these observations suggest a role of the glucoside transporters in proper function of the SepJ-related septal junctions. GFP fusions indicate that GlsC, GlsP and HepP are located in the periphery of the cells including the intercellular septa (Figs. 4 and S6 and ref. 36), where they could interact with the septal junction complexes. To investigate whether such interactions are feasible, BACTH analysis was carried out with the glucoside transporter proteins and SepJ. This analysis showed that GlsP and, most strongly, HepP can interact with SepJ, whereas no interaction was observed between SepJ and GlsC. Hence, GlsP and HepP may affect SepJ function by means of protein-protein interactions. A functional dependence between SepJ and an ABC transporter for polar amino acids has also been described (57). These observations suggest that proper operation of SepJ, and hence of the SepJ-related septal junctions, requires interaction with other cytoplasmic membrane proteins.

GlsC is instead required for proper location of SepJ and maturation of the intercellular septa, as illustrated by the presence of a lower number of nanopores in the *glsC* mutant than in the wild type. How GlsC influences SepJ localization and nanopore formation is unknown, but we note (i) that an N-acetylmuramoyl-L-alanine amidase, AmiC, is required for drilling the septal peptidoglycan nanopores (19) and (ii) that the presence of septal proteins including SepJ is needed for the amidase to make the nanopores (18). In other bacteria, the ABC transporter-like FtsEX complex, in which FtsE is an ATP-binding subunit, is required for activation of amidases that split the septal peptidoglycan during cell division (58, 59) and of endopeptidases that function in cell elongation (60, 61). An appealing hypothesis

615 is that GlsC participates in an ABC transporter-like complex that regulates amidases involved in nanopore
616 formation with an effect on localization of SepJ.

617 The different effects of inactivation of *glsC* –impairment of esculin uptake and alteration of septal
618 structure– indicate that GlsC has multiple functions. Multitask ATP-binding subunits that serve different
619 ABC transporters have been described, e.g., in *Streptomyces lividans* (62), *Streptococcus mutans* (63),
620 *Bacillus subtilis* (64) and *Corynebacterium alkanolyticum* (65), as well as in *Anabaena* (66). As checked
621 at the Integrated Microbial Genomes webpage (https://img.jgi.doe.gov/cgi-bin/m/main.cgi), the *glsC* gene
622 is not clustered with any other gene encoding an ABC transporter component in any cyanobacterium
623 whose genome sequence is available. Therefore, no preferential association of GlsC to any particular
624 ABC transporter can be established based on genomic data. Nonetheless, in a few cases the neighboring
625 genes are related to cell wall biosynthesis, including an N-acetylmuramoyl-L-alanine amidase-encoding
626 gene in *Spirulina major* PCC 6313, consistent with the idea of a relation of GlsC to cell wall maturation.

627 In summary, we have identified three genes encoding components of transporters that mediate α-
628 glucoside uptake, including sucrose uptake, in *Anabaena*. These transporters appear to influence septal
629 junction maturation –in the case of *glsC*– or function –in the case of *glsP* and *hepP*. As a consequence,
630 inactivation of these genes impairs molecular transfer between vegetative cells negatively affecting
631 diazotrophy. A major task for future research is to explore whether the interplay between these
632 transporters and SepJ has a function regulating the activity of septal junctions.
633

ACKNOWLEDGMENTS

We thank Antonia Herrero (Sevilla) for useful discussions, Alexandra Johnson (East Lansing) for her cloning work related to generation of DR3912a and DR3915, and Sergio Camargo (Sevilla) for help with the immunofluorescence and RT-qPCR analyses. MN-M was the recipient of a FPU (Formación de Profesorado Universitario) fellowship/contract from the Spanish Government.

FUNDING INFORMATION

Work in Seville was supported by grant no. BFU2014-56757-P from Plan Nacional de Investigación, Spain, co-financed by the European Regional Development Fund. Work in East Lansing was supported by the Biosciences Division, Office of Basic Energy Sciences, Office of Science, U.S. Department of Energy (grant DOE FG02-91ER20021).

REFERENCES

1. **Flores E, Herrero A.** 2014. The cyanobacteria: morphological diversity in a photoautotrophic lifestyle. Perspectives in Phycology **1:**63-72.
2. **Wolk CP.** 1996. Heterocyst formation. Annu Rev Genet **30:**59–78.
3. **Wolk CP, Ernst A, Elhai J.** 1994. Heterocyst metabolism and development, p 769–823. *In* Bryant DA (ed), The Molecular Biology of Cyanobacteria. Kluwer Academic Publishers, Dordrecht.
4. **Herrero A, Stavans J, Flores E.** 2016. The multicellular nature of filamentous heterocyst-forming cyanobacteria. FEMS Microbiol Rev **40:**831-854.
5. **Flores E, Herrero A, Wolk CP, Maldener I.** 2006. Is the periplasm continuous in filamentous multicellular cyanobacteria? Trends Microbiol **14**:439-443.
6. **Mariscal V, Herrero A, Flores E.** 2007. Continuous periplasm in a filamentous, heterocyst-forming cyanobacterium. Mol Microbiol **65**:1139-1145.
7. **Mullineaux CW, Mariscal V, Nenninger A, Khanum H, Herrero A, Flores E, Adams DG.** 2008. Mechanism of intercellular molecular exchange in heterocyst-forming cyanobacteria. EMBO J **27**:1299-1308.
8. **Mariscal V.** 2014. Cell-cell joining proteins in heterocyst-forming cyanobacteria, p 293-304. *In* Flores E, Herrero A (eds), The Cell Biology of Cyanobacteria. Caister Academic Press, Norfolk, UK.
9. **Mullineaux CW, Nürnberg DJ.** 2014. Tracing the path of a prokaryotic paracrine signal. Mol Microbiol **94**:1208-1212.
10. **Flores E, Herrero A, Forchhammer K, Maldener I.** 2016. Septal junctions in filamentous heterocyst-forming cyanobacteria. Trends Microbiol **24**:79-82.
11. **Erickson RO.** 1986. Symplastic growth and symplasmic transport. Plant Physiol **82:**1153.
12. **Flores E, Pernil R, Muro-Pastor AM, Mariscal V, Maldener I, Lechno-Yossef S, Fan Q, Wolk CP, Herrero A.** 2007. Septum-localized protein required for filament integrity and diazotrophy in the heterocyst-forming cyanobacterium *Anabaena* sp. strain PCC 7120. J Bacteriol **189**:3884-3890.
13. **Merino-Puerto V, Mariscal V, Mullineaux CW, Herrero A, Flores E.** 2010. Fra proteins influencing filament integrity, diazotrophy and localization of septal protein SepJ in the heterocyst-forming cyanobacterium *Anabaena* sp. Mol Microbiol **75**:1159-1170.
14. **Merino-Puerto V, Schwarz H, Maldener I, Mariscal V, Mullineaux CW, Herrero A, Flores E.** 2011. FraC/FraD-dependent intercellular molecular exchange in the filaments of a heterocyst-forming cyanobacterium, *Anabaena* sp. Mol Microbiol **82**:87-98.
15. **Ramos-León F, Mariscal V, Frías JE, Flores E, Herrero A.** 2015. Divisome-dependent subcellular localization of cell-cell joining protein SepJ in the filamentous cyanobacterium *Anabaena*. Mol Microbiol **96:**566-580.
16. **Rudolf M, Tetik N, Ramos-León F, Flinner N, Ngo G, Stevanovic M, Burnat M, Pernil R, Flores E, Schleiff E.** 2015. The peptidoglycan-binding protein SjcF1 influences septal junction function and channel formation in the filamentous cyanobacterium *Anabaena*. mBio **6(4):**e00376-15.
17. **Mariscal V, Herrero A, Nenninger A, Mullineaux CW, Flores E.** 2011. Functional dissection of the three-domain SepJ protein joining the cells in cyanobacterial trichomes. Mol Microbiol **79**:1077-1088.
18. **Nürnberg DJ, Mariscal V, Bornikoel J, Nieves-Morión M, Krauß N, Herrero A, Maldener I, Flores E, Mullineaux CW.** 2015. Intercellular diffusion of a fluorescent sucrose analog via the septal junctions in a filamentous cyanobacterium. mBio **6(2):**e02109.

19. **Lehner J, Berendt S, Dörsam B, Pérez R, Forchhammer K, Maldener I.** 2013. Prokaryotic multicellularity: a nanopore array for bacterial cell communication. FASEB J **27**:2293-30.
20. **Omairi-Nasser A, Mariscal V, Austin JR 2nd, Haselkorn, R.** 2015. Requirement of Fra proteins for communication channels between cells in the filamentous nitrogen-fixing cyanobacterium *Anabaena* sp. PCC 7120. Proc Natl Acad Sci USA **112(32):**E4458-E4464.
21. **Schilling N, Ehrnsperger K.** 1985. Cellular differentiation of sucrose metabolism in *Anabaena variabilis*. Z Naturforsch **40c**:776-779.
22. **Curatti L, Flores E, Salerno G.** 2002. Sucrose is involved in the diazotrophic metabolism of the heterocyst-forming cyanobacterium *Anabaena* sp. FEBS Lett **513**:175-178.
23. **López-Igual R, Flores E, Herrero A.** 2010. Inactivation of a heterocyst-specific invertase indicates a principal role of sucrose catabolism in the heterocysts of *Anabaena* sp. J Bacteriol **192**:5526–5533.
24. **Vargas WA, Nishi CN, Giarrocco LE, Salerno GL.** 2011. Differential roles of alkaline/neutral invertases in *Nostoc* sp. PCC 7120: Inv-B isoform is essential for diazotrophic growth. Planta **233**:153-162.
25. **Kolman MA, Nishi CN, Perez-Cenci M, Salerno GL.** 2015. Sucrose in cyanobacteria: from a salt-response molecule to play a key role in nitrogen fixation. Life (Basel) **5:**102-126.
26. **Nieves-Morión M, Mullineaux CW, Flores E.** 2017. Molecular diffusion through cyanobacterial septal junctions. mBio **8:**e01756-16.
27. **Stebegg R, Wurzinger B, Mikulic M, Schmetterer G.** 2012. Chemoheterotrophic growth of the cyanobacterium *Anabaena* sp. strain PCC 7120 dependent on a functional cytochrome *c* oxidase. J Bacteriol **194:**4601-4607.
28. **Rippka R, Deruelles J, Waterbury JB, Herdman M, Stanier RY.** 1979. Generic assignments, strain histories and properties of pure cultures of cyanobacteria. J Gen Microbiol **111**:1-61.
29. **Hu N-T, Thiel T, Giddings TH, Wolk CP.** 1981. New *Anabaena* and *Nostoc* cyanophages from sewage settling ponds. Virology **114:**236–246.
30. **Mackinney G.** 1941. Absorption of light by chlorophyll solutions. J Biol Chem **140**:315-322.
31. **Ausubel FM, Brent R, Kingston RE, Moore DD, Seidman JG, Smith JA, Struhl K.** 2014. Current Protocols in Molecular Biology. Greene Publishing and Wiley-Interscience, New York.
32. **Elhai J, Vepritskiy A, Muro-Pastor AM, Flores E, Wolk CP.** 1997. Reduction of conjugal transfer efficiency by three restriction activities of *Anabaena* sp. strain PCC 7120. J Bacteriol **179**:1998-2005.
33. **Cai Y, Wolk CP.** 1990. Use of a conditionally lethal gene in *Anabaena* sp. strain PCC 7120 to select for double recombinants and to entrap insertion sequences. J Bacteriol **172**:3138-3145.
34. **Wolk CP, Cai Y, Cardemil L, Flores E, Hohn B, Murry M, Schmetterer G, Schrautemeier B, Wilson R.** 1988. Isolation and complementation of mutants of *Anabaena* sp. strain PCC 7120 unable to grow aerobically on dinitrogen. J Bacteriol **170:**1239-1244.
35. **Valladares A, Rodríguez V, Camargo S, Martínez-Noël GM, Herrero A, Luque I.** 2011. Specific role of the cyanobacterial PipX factor in the heterocysts of *Anabaena* sp. strain PCC 7120. J Bacteriol **193:**1172-1182.
36. **López-Igual R, Lechno-Yossef S, Fan Q, Herrero A, Flores E, Wolk CP.** 2012. A major facilitator superfamily protein, HepP, is involved in formation of the heterocyst envelope polysaccharide in the cyanobacterium *Anabaena* sp. strain PCC 7120. J Bacteriol **194:**4677-4687.
37. **Black TA, Cai Y, Wolk CP.** 1993. Spatial expression and autoregulation of *hetR*, a gene involved in the control of heterocyst development in *Anabaena*. Mol Microbiol **9**:77-84 Publisher's correction (1993): Mol Microbiol **10**:1153.

38. **Cormack BP, Valdivia RH, Falkow S.** 1996. FACS-optimized mutants of the green fluorescent protein (GFP). Gene **173:**33-38.
39. **Livak KJ, Schmittgen TD.** 2001. Analysis of relative gene expression data using real-time quantitative PCR and the 2(-Delta Delta C(T)) method. Methods **25**:402-408.
40. **Krzywinski M, Altman N.** 2014. Visualizing samples with box plots. Nat Methods **11:**119-120.
41. **Gora PJ, Reinders A, Ward JM.** 2012. A novel fluorescent assay for sucrose transporters. Plant Methods **8**:13.
42. **Park J-J, Lechno-Yossef, S, Wolk CP, Vieille C.** 2013. Cell-specific gene expression in *Anabaena variabilis* grown phototrophically, mixotrophically and heterotrophically. BMC Genomics **14**: 759.
43. **Kaneko T, Nakamura, Y, Wolk CP, Kuritz T, Sasamoto S, Watanabe A, Iriguchi M, Ishikawa A, Kawashima K, Kimura T, Kishida Y, Kohara M, Matsumoto M, Matsuno A, Muraki A, Nakazaki N, Shimpo S, Sugimoto M, Takazawa M, Yamada M, Yasuda M, Tabata S.** 2001. Complete genomic sequence of the filamentous nitrogen-fixing cyanobacterium *Anabaena* sp. strain PCC 7120. DNA Res **8**:205-213.
44. **Elhai J, Wolk CP.** 1988. A versatile class of positive-selection vectors based on the nonviability of palindrome-containing plasmids that allows cloning into long polylinkers. Gene **68**:119-138.
45. **Cui J, Davidson AL.** 2011. ABC solute importers in bacteria. Essays Biochem **50:**85-99.
46. **Drew D, Sjöstrand D, Nilsson J, Urbig T, Chin CN, de Gier JW, von Heijne G.** 2002. Rapid topology mapping of *Escherichia coli* inner-membrane proteins by prediction and PhoA/GFP fusion analysis. Proc Natl Acad Sci USA 99:2690-2695.
47. **McKinney RE.** 1953. Staining bacterial polysaccharides. J Bacteriol **66:**453-454.
48. **Karimova G, Pidoux J, Ullmann A, Ladant D.** 1998. A bacterial two-hybrid system based on a reconstituted signal transduction pathway. Proc Natl Acad Sci USA 95:5752-5756.
49. **Battesti A, Bouveret E.** 2012. The bacterial two-hybrid system based on adenylate cyclase reconstitution in Escherichia coli. Methods **58:**325-334.
50. **Stynen B, Tournu H, Tavernier J, Van Dijck P.** 2012. Diversity in genetic in vivo methods for protein-protein interaction studies: from the yeast two-hybrid system to the mammalian split-luciferase system. Microbiol Mol Biol Rev **76:**331-382.
51. **Flaherty BL, van Nieuwerburgh F, Head SR, Golden JW.** 2011. Directional RNA deep sequencing sheds new light on the transcriptional response of *Anabaena* sp. strain PCC 7120 to combined-nitrogen deprivation. BMC Genomics **12:**332.
52. **Nicolaisen K, Mariscal V, Bredemeier R, Pernil R, Moslavac S, López-Igual R, Maldener I, Herrero A, Schleiff E, Flores E.** 2009. The outer membrane is a permeability barrier for intercellularly exchanged metabolites in a heterocyst-forming cyanobacterium. Mol Microbiol **74:**58-70.
53. **Reinders A, Sivitz AB, Ward JM.** 2012. Evolution of plant sucrose uptake transporters. Front Plant Sci **3:**22.
54. **Stuart RK, Mayali X, Lee JZ, Craig Everroad R, Hwang M, Bebout BM, Weber PK, Pett-Ridge J, Thelen MP.** 2015. Cyanobacterial reuse of extracellular organic carbon in microbial mats. ISME J **10:**1240-1251.
55. **Ungerer JL, Pratte BS, Thiel T.** 2008. Regulation of fructose transport and its effect on fructose toxicity in *Anabaena* spp. J Bacteriol **190:**8115-8125.
56. **Ayre BG**. 2011. Membrane-transport systems for sucrose in relation to whole-plant carbon partitioning. Mol Plant **4:**377-394.

57. **Escudero L, Mariscal V, Flores E.** 2015. Functional dependence between septal protein SepJ from *Anabaena* sp. strain PCC 7120 and an amino acid ABC-type uptake transporter. J Bacteriol **197:**2721-2730.
58. **Yang DC, Peters NT, Parzych KR, Uehara T, Markovski M, Bernhardt TG.** 2011. An ATP-binding cassette transporter-like complex governs cell-wall hydrolysis at the bacterial cytokinetic ring. Proc Natl Acad Sci USA **108:** E1052-1060.
59. **Bartual SG, Straume D, Stamsås GA, Muñoz IG, Alfonso C, Martínez-Ripoll M, Håvarstein LS, Hermoso JA.** 2014. Structural basis of PcsB-mediated cell separation in *Streptococcus pneumoniae*. Nat Commun **5:** 3842.
60. **Domínguez-Cuevas P, Porcelli I, Daniel RA, Errington J.** 2013. Differentiated roles for MreB-actin isologues and autolytic enzymes in *Bacillus subtilis* morphogenesis. Mol Microbiol **89:**1084-1098.
61. **Meisner J, Montero Llopis, P, Sham LT, Garner E, Bernhardt TG, Rudner DZ.** 2013. FtsEX is required for CwlO peptidoglycan hydrolase activity during cell wall elongation in *Bacillus subtilis*. Mol Microbiol **89:**1069-83.
62. **Schlösser A, Kampers T, Schrempf H.** 1997. The *Streptomyces* ATP-binding component MsiK assists in cellobiose and maltose transport. J Bacteriol **179:**2092-2095.
63. **Webb AJ, Homer KA, Hosie AH. 2008.** Two closely related ABC transporters in *Streptococcus mutans* are involved in disaccharide and/or oligosaccharide uptake. J Bacteriol **190:**168-178.
64. **Ferreira MJ, de Sá-Nogueira I.** 2010. A multitask ATPase serving different ABC-type sugar importers in *Bacillus subtilis*. J Bacteriol **192:**5312-5318.
65. **Watanabe A, Hiraga K, Suda M, Yukawa H, Inui M.** 2015. Functional characterization of *Corynebacterium alkanolyticum* β-xylosidase and xyloside ABC transporter in *Corynebacterium glutamicum*. Appl Environ Microbiol **81:**4173-4183.
66. **Pernil R, Picossi S, Mariscal V, Herrero A, Flores E.** 2008. ABC-type amino acid uptake transporters Bgt and N-II of *Anabaena* sp. strain PCC 7120 share an ATPase subunit and are expressed in vegetative cells and heterocysts. Mol Microbiol **67:**1067-1080.

806 **Figure legends**

807

808 **Figure 1.** Effect of concentration of esculin on the uptake of esculin by *Anabaena*. BG11-grown
809 filaments or filaments grown in BG11 medium and incubated for 18 h in $BG11_0$ medium were
810 resuspended in the same media supplemented with 10 mM HEPES-NaOH (pH 7) and used in uptake
811 assays with the indicated concentrations of esculin as described in Materials and Methods. Error bars refer
812 to standard deviations (SD); n = 3.

813 **Figure 2.** Effect of pH on the uptake of esculin by *Anabaena*. Filaments were grown in BG11 medium
814 and were then either resuspended in BG11 medium, or were incubated for 18 h in $BG11_0$ medium and
815 then resuspended in $BG11_0$ medium. Both media were supplemented with 10 mM HEPES-NaOH at the
816 indicated values of pH and were used in assays of uptake with 100 μM esculin as described in Materials
817 and Methods. The differences of the mean values of uptake of esculin between filaments resuspended in
818 $BG11_0$ and BG11 at the different values of pH tested were represented as $BG11_0$-BG11. Error bars, SD.
819 For pH 7, n = 25 (BG11) or 20 ($BG11_0$); for all other values of pH, n = 3.

820 **Figure 3.** Effect of sugars on the uptake of esculin by *Anabaena*. BG11-grown filaments or filaments
821 grown in BG11 medium and incubated for 18 h in $BG11_0$ medium were resuspended in the same media
822 supplemented with 10 mM HEPES-NaOH (pH 7) and the indicated sugar at 1 mM. No add., no sugar
823 added; Suc, sucrose; Mal, maltose; Tre, trehalose; Lac, lactose; Glc, glucose; Frc, fructose; Gal, galactose.
824 The assays were performed with 100 μM esculin as described in Materials and Methods. Error bars, SD; n
825 = 2-3, except for No add., 25 (BG11) or 20 ($BG11_0$). Asterisks denote significant differences in
826 comparison to the assays without added sugars in BG11 or $BG11_0$ medium (Student's *t* test, $P < 0.05$).

827 **Figure 4.** Subcellular localization of GlsC-GFP and GlsP-GFP. Filaments of strains CSMN13 (*glsC*::*gfp*)
828 and CSMN15 (*glsP*::*gfp*) grown in BG11 medium in the presence of antibiotics were incubated in BG11
829 or $BG11_0$ medium without antibiotics for 24 h. GFP fluorescence was visualized by confocal microscopy

as described in Materials and Methods. Brightness and contrast were enhanced to improve visibility. Arrows point to heterocysts. Size bars, 10 µm.

Figure 5. Tests of growth on solid medium of wild-type *Anabaena*, and the *glsC* (DR3912a), *glsP* (DR3915), and *glsC glsP* (DR3912a DR3985a) mutants. Filaments grown in BG11 medium (in the presence of antibiotics for the mutants) were resuspended in $BG11_0$ medium, dilutions were prepared, and a 10-µl portion of each dilution (from left to right: 1, 0.5, 0.25, 0.125 and 0.0625 µg Chl ml^{-1}) was spotted on BG11 (NO_3^-) or $BG11_0$ (N_2) medium. The plates were incubated under culture conditions, and photographs taken after 7 and 11 days of incubation are shown to help appreciate the growth-defect phenotypes.

Figure 6. Heterocysts in the *glsC glsP* double mutant. Filaments of the the wild type (PCC 7120) and of the double mutant grown in BG11 medium (in the presence of antibiotics for the mutant) were inoculated in liquid $BG11_0$ medium without antibiotics and incubated four days under culture conditions. Staining with Alcian Blue was done as described in Materials and Methods, and the filament suspensions were observed by light microscopy. Black arrows point to some stained heterocysts. Scale bars, 10 mm.

Figure 7. Subcellular localization of SepJ-GFP in the wild-type and transporter mutant genetic backgrounds. Filaments of strains CSAM137 (PCC 7120 [*sepJ*::pCSAM137]), CSMN9 (*glsC*::C.S3 *sepJ*::pCSVT22), CSMN10 (*glsP*::C.S3 *sepJ*::pCSVT22), and CSMN16 (*hepP*::Tn1063 *sepJ*::pCSAM137) were grown in BG11 medium in the presence of antibiotics and visualized by confocal microscopy as described in Materials and Methods. Size bars, 10 mm. In the *hepP* mutant SepJ is seen localized in the middle of many cells; these cells are likely starting cell division, and SepJ is known to localize to the cell division site when cell division starts (12, 15).

Figure 8. Immunofluorescence localization of SepJ in *Anabaena* (PCC 7120) and strains *glsC* and *glsC-C.* Filaments of strains PCC 7120, DR3912a (*glsC*::C.S3), and DR3912a [pCSMN22] (*glsC*::C.S3, *glsC*) were grown in BG11 medium in the presence of antibiotics for the mutants and subjected to

immunoflurescence analysis with anti SepJ coiled-coil antibodies as described in Materials and Methods. Overlay images of antibody green fluorescence and cyanobacterial autofluorescence are shown. Size bars, 10 mm.

Figure 9. Septal peptidoglycan disk nanopores in wild-type *Anabaena* and mutants. (A) Murein sacculi were isolated from strains PCC 7120 (WT), DR3912a (*glsC*::C.S3), DR3915 (*glsP*::C.S3) and FQ163 (*hepP*::Tn5-1063) grown in BG11 medium and visualized by transmission electron microscopy. (B) Quantification of nanopores in disks from the indicated strains (mean and SD; n, number of disks counted). WT versus *glsC*, Student's *t* test $P = 0.002$.

TABLE 1 Esculin uptake in *Anabaena* and some mutant strains.

Strain	Genotype	Product of the mutated gene(s)	Esculin uptake (nmol [mg Chl]$^{-1}$ min^{-1}) [a]			
			BG11		$BG11_0$	
			Mean ± SD (n)	% of WT (*P*)	Mean ± SD (n)	% of WT (*P*)
PCC 7120	WT		0.161 ± 0.059 (25)		0.298 ± 0.085 (20)	
DR3912a	*alr4781*::C.S3	GlsC	0.079 ± 0.037 (10)	49% (0.0003)	0.220 ± 0.065 (9)	74% (0.021)
DR3915	*all0261*::C.S3	GlsP	0.095 ± 0.041 (10)	59% (0.003)	0.217 ± 0.089 (9)	73% (0.027)
DR3985a-DR3912a	*all0261*::C.CE *alr4781*::C.S3	GlsC, GlsP	0.041 ± 0.020 (10)	25% (10^{-6})	0.149 ± 0.024 (5)	50% (0.007)
CSRL15	*alr3705*::C.S3	MFS permease	0.181 ± 0.067 (3)	112% (0.591)	0.339 ± 0.073 (4)	113% (0.383)
FQ163	*all1711*::Tn5-1063	HepP	0.174 ± 0.076 (4)	108% (0.703)	0.206 ± 0.020 (4)	69% (0.046)
CSMN3	*alr3705*::C.S3 *all1711*::Tn5-1063	MFS permease, HepP	0.139 ± 0.058 (3)	86% (0.553)	0.200 ± 0.042 (4)	67% (0.037)

[a] Filaments grown in BG11 medium (in the presence of antibiotics for the mutants) were washed and resuspended in BG11 or $BG11_0$ media without antibiotics and incubated for 18 h under culture conditions. Filaments were then resuspended in the same media supplemented with 10 mM HEPES-NaOH (pH 7) and used in assays of uptake of 100 μM esculin as described in Materials and Methods. Data are mean and SD of the indicated number of assays performed with independent cultures. Significance of the difference between each mutant and the wild type was assessed by the Student's *t* test; *P* is indicated in each case.

TABLE 2 Growth rates, heterocysts and nitrogenase activity in *Anabaena* and ABC transporter mutant strains.

Strain (mutated genes)	Growth rate constant (μ, day^{-1}; mean ± SD) [a]		Heterocysts (%) [b]	Nitrogenase activity (nmol ethylene produced [μg Chl]$^{-1}$ h^{-1}; mean ± SD) [c]	
	BG11	$BG11_0$	48 h –N	Oxic	Anoxic
PCC 7120 (WT)	0.67 ± 0.07 (5)	0.49 ± 0.09 (5)	9.33 %	23.37 ± 5.17 (4)	10.54 ± 3.05 (3)
DR3912a (*glsC*)	0.67 ± 0.14 (5)	0.28 ± 0.15 (5)	5.58 %	2.52 ± 1.89 (3)	2.47 ± 0.15 (2)
DR3915 (*glsP*)	0.67 ± 0.07 (5)	0.36 ± 0.08 (5)	7.93 %	2.13 ± 0.63 (3)	3.00 ± 1.48 (2)
DR3912a-DR3985a (*glsC glsP*) [d]	0.50 ± 0.10 (5)	0.06 ± 0.07 (5)	2.22 %	1.53 ± 1.61 (8)	2.08 ± 1.70 (6)

[a] Growth rate constants were determined in BG11 or $BG11_0$ liquid media as described in Materials and Methods for the number of independent cultures shown in parenthesis. The difference between the *glsC glsP* mutant and the WT was significant in BG11 (Student's *t* test $P = 0.014$) and $BG11_0$ ($P < 0.001$) media; the differences were also significant between *glsC* and WT ($P = 0.029$) and between *glsP* and WT ($P = 0.045$) in $BG11_0$ medium.

[b] Filaments of the indicated strains grown in BG11 medium (with antibiotics for the mutants) and incubated in $BG11_0$ medium without antibiotics for 48 h were used to determine the percentage of heterocysts (about 1,500 cells counted for each strain).

[c] Filaments of the indicated strains grown in BG11 medium (with antibiotics for the mutants) and incubated in $BG11_0$ medium without antibiotics for 48 h were used to determine nitrogenase activity. Acetylene reduction was assayed under oxic and anoxic conditions (see Materials and Methods); the differences were significant for all the mutants vs. the WT (Student's *t* test $P < 0.002$ [oxic conditions] and ≤ 0.05 [anoxic conditions]). The number of determinations done with independent cultures is indicated in parenthesis.

[d] After 48 h of incubation in $BG11_0$ medium, the filaments of this strain were extensively fragmented (see the text). Those filaments containing heterocysts also contained a mean of 5.4 vegetative cells per filament.

TABLE 3 Transfer of esculin between vegetative cells or from vegetative cells to heterocysts in *Anabaena* and glucoside transporter mutant strains.

Strain (mutated genes)	**Esculin transfer (*R*, s^{-1})[a]**					
	BG11-grown filaments		**Filaments incubated in $BG11_0$ medium**			
	Vegetative cells		**Vegetative cells**		**Heterocysts**	
	Mean ± SD (n)	% of WT (*P*)	Mean ± SD (n)	% of WT (*P*)	Mean ± SD (n)	% of WT (*P*)
PCC 7120 (WT)	0.157 ± 0.052 (49)		0.162 ± 0.062 (60)		0.060 ± 0.067 (82)	
DR3912a (*glsC*)	0.122 ± 0.051 (77)	78% ($< 10^{-3}$)	0.047 ± 0.048 (28)	29% ($< 10^{-12}$)	0.074 ± 0.081 (55)	123% (0.277)
DR3915 (*glsP*)	0.144 ± 0.054 (43)	92% (0.200)	0.094 ± 0.077 (25)	58% ($< 10^{-4}$)	0.091 ± 0.084 (33)	152% (0.060)
DR3912a, DR3985a (*glsC glsP*)	0.105 ± 0.042 (55)	67% ($< 10^{-6}$)	0.094 ± 0.070 (37)	58% ($< 10^{-5}$)	0.088 ± 0.057 (25)	147% (0.070)
FQ163 (*hepP*)	0.090 ± 0.058 (56)	57% ($< 10^{-4}$)	0.068 ± 0.051 (17)	42% ($< 10^{-10}$)	0.156 ± 0.082 (27)	260% (10^{-8})

[a] Filaments of the wild type and the indicated mutants grown in BG11 medium (with antibiotics for the mutants) and incubated in BG11 medium without antibiotics for 18 to 24 h or in $BG11_0$ medium without antibiotics for 48 h were used in FRAP analysis as described in Materials and methods. Data are mean ± SD from the results obtained with the indicated number of filaments (n) subjected to FRAP analysis. Filaments from two to six independent cultures were used. Student's *t* test (mutant vs. wild type) *P* is indicated in each case.

Table 4 Transfer of calcein and 5-CF between nitrate-grown vegetative cells in *Anabaena* and glucoside transporter mutant strains[a].

Strain (mutated genes)	**Calcein transfer (*R*, s^{-1})**		**5-CF transfer (*R*, s^{-1})**	
	Mean ± SD (n)	% of WT (*P*)	Mean ± SD (n)	% of WT (*P*)
PCC 7120 (WT)	0.070 ± 0.053 (50)		0.087 ± 0.045 (136)	
DR3912a (*glsC*)	0.039 ± 0.033 (47)	55% (< 10^{-3})	0.069 ± 0.060 (105)	79% (0.009)
DR3915 (*glsP*)	0.028 ± 0.041 (68)	39% (< 10^{-5})	0.059 ± 0.059 (96)	68% (< 10^{-4})
DR3912a, DR3985a (*glsC glsP*)	0.015 ± 0.020 (43)	21% (< 10^{-8})	0.064 ± 0.054 (48)	74% (0.004)
FQ163 (*hepP*)	0.022 ± 0.027 (33)	31% (< 10^{-5})	0.082 ± 0.044 (27)	94% (0.604)

[a] Filaments of the wild type and the indicated mutants grown in BG11 medium (with antibiotics for the mutants) and incubated in BG11 medium without antibiotics for 18 to 24 h were used in FRAP analysis as described in Materials and Methods. Data are mean ± SD from the results obtained with the indicated number of filaments (n) subjected to FRAP analysis. Filaments from two to six (calcein) or up to 9 (5-CF) independent cultures were used. Student's *t* test (mutant vs. wild type) *P* is indicated in each case.

Table 5 Bacterial two-hybrid analysis of protein-protein interactions[a].

	T18	*SepJ-T18*	*GlsC-T18*	*T18-GlsC*	*GlsP-T18*	*T18-GlsP*	*HepP-T18*	*T18-HepP*
T25	12.66 ± 2.34 (9)	10.88 ± 1.06 (6)	13.01 ± 3.49 (4)	12.34 ± 0.80 (4)	12.11 ± 4.10 (4)	10.95 ± 3.37 (4)	12.12 ± 1.33 (4)	11,99 ± 2,69 (4)
SepJ-T25	11.22 ± 2.04 (2)	**** 80.12 ± 37.03 (9)**	13.25 ± 2.91 (5)	15.75 ± 11.31 (3)	11.74 ± 3.68 (5)	14.66 ± 2.12 (4)	11.42 ± 1.36 (4)	**** 28.35 ± 5.93 (4)**
GlsC-T25	Nd	11.66 ± 1.99 (6)	12.52 ± 3.32 (4)	*** 20.52 ± 4.90 (4)**	12.36 ± 0.95 (3)	13 ± 5.72 (3)	12.27 ± 3.61 (3)	12.11 ± 1.48 (4)
T25-GlsC	Nd	13.09 ± 3.06 (6)	**** 25.98 ± 5.46 (4)**	15.93 ± 6.35 (6)	12.72 ± 3.11 (4)	12.79 ± 3.73 (3)	13.57 ± 1.92 (4)	11.98 ± 0.86 (4)
GlsP-T25	Nd	14.34 ± 2.22 (7)	12.32 ± 3.11 (5)	14.19 ± 7.44 (4)	12.16 ± 2.11 (4)	11.64 ± 4.06 (3)	13.13 ± 2.23 (4)	17.44 ± 4.70 (4)
T25-GlsP	Nd	**** 29.12 ± 9.36 (7)**	11.80 ± 2.27 (5)	15.48 ± 8.28 (4)	11.85 ± 0.55 (3)	12.04 ± 6.11 (3)	13.63 ± 1.47 (4)	*** 23.08 ± 7.03 (4)**
HepP-T25	10.58 ± 4.35 (4)	12.96 ± 3.26 (4)	12.83 ± 1.50 (4)	12.08 ± 1.12 (4)	13.94 ± 2.29 (4)	13.65 ± 2.48 (4)	13.86 ± 1.37 (4)	16.73 ± 8.38 (4)
T25-HepP	13.60 ± 2.01 (4)	**** 75.31 ± 6.74 (4)**	14.56 ± 2.47 (4)	13.06 ± 2.81 (4)	18.33 ± 2.50 (4)	**** 34.16 ± 7.18 (4)**	13.77 ± 0.99 (4)	**** 79.97 ± 22.12 (4)**

[a] Interactions of T25- and T18-fusion proteins produced in *E. coli* were measured as β-galactosidase activity in liquid cultures. Activity corresponds to nmol *o*-nitrophenol (mg protein)$^{-1}$ min^{-1}. The protein fused to the N- or the C-terminus of T18 or T25 is indicated in each case (N-terminus, protein-T18 or protein-T25; C-terminus, T18-protein or T25-protein). The mean and standard deviation of the results obtained with the indicated number of independent transformants (n) is presented. The difference between each fusion protein combination and the T18/T25 pair was assessed by the Student's *t* test; bold type denotes significant differences (*, $P \leq 0.005$; **, $P \leq 0.001$). All other combinations gave activities not significantly different from the T25/T18 control, $P > 0.05$. Nd, not determined.

Fig. 1

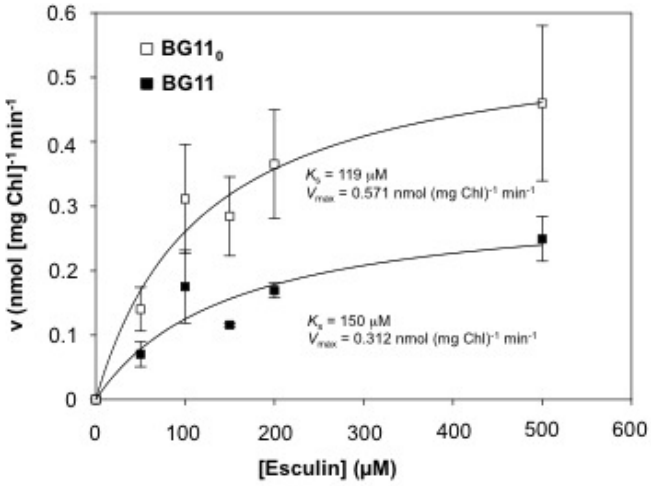

Fig. 2

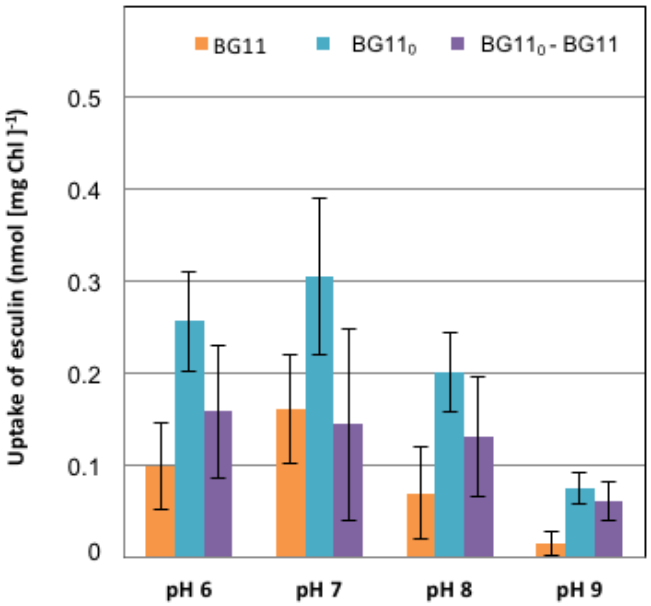

Fig. 3

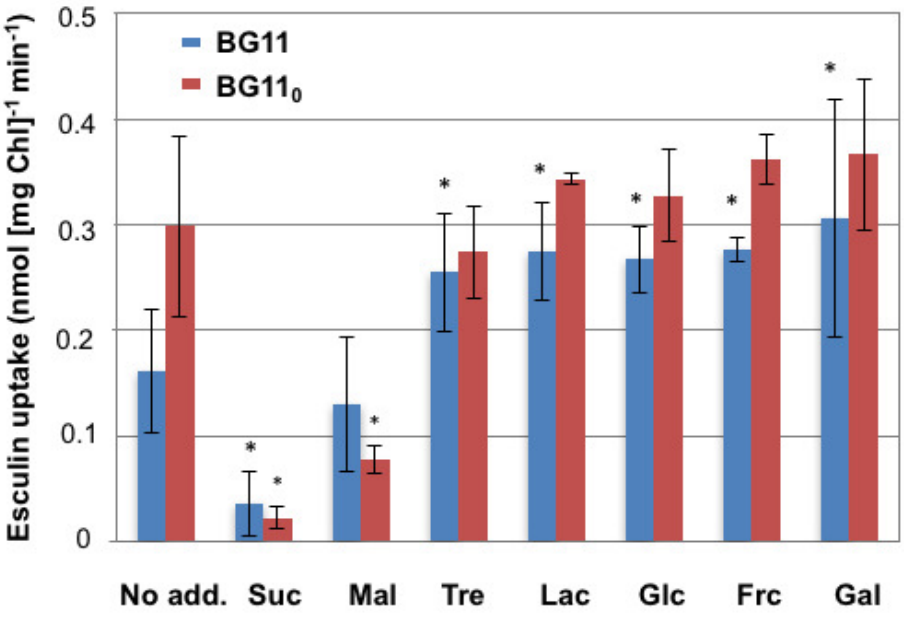

Fig. 4

Fig. 5

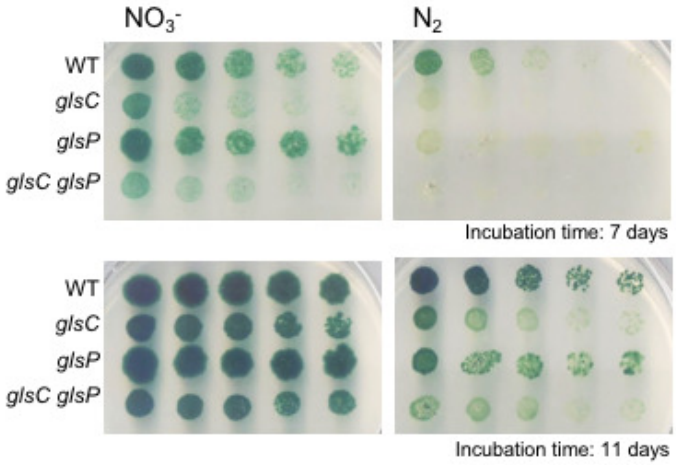

Fig. 6

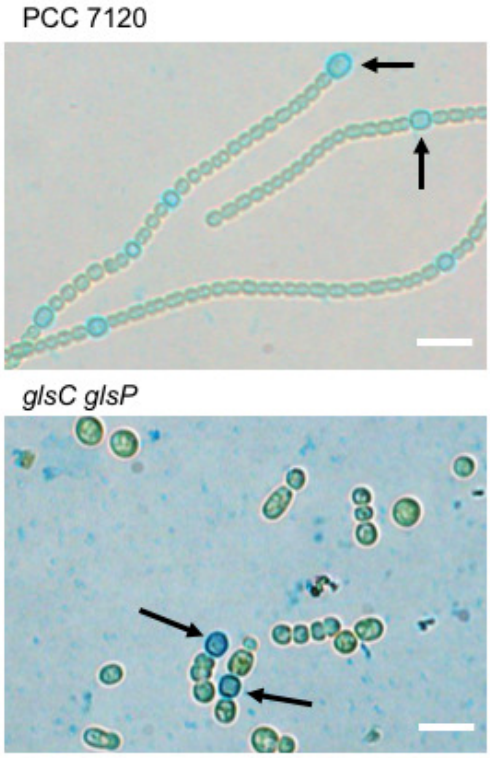

Fig. 7

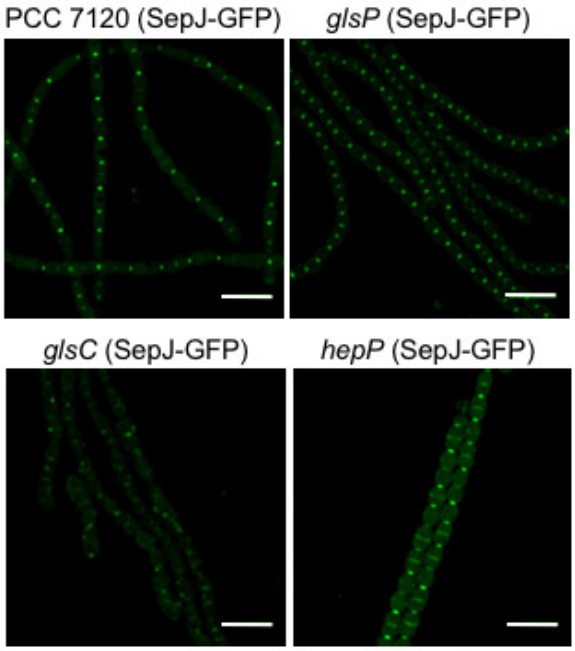

Fig. 8

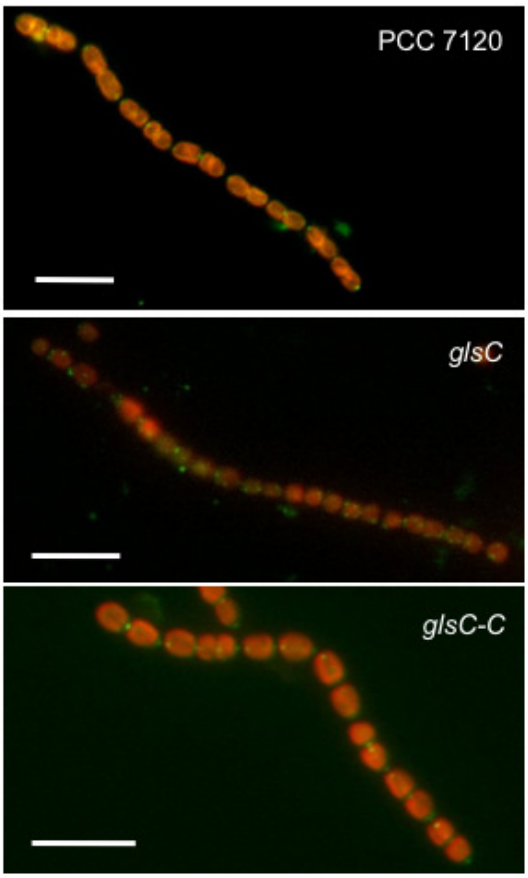

Fig. 9